

---

PAPER

## Electromechanical enhancement of metal nanoparticle thin film by composite formation with short metal nanowires

To cite this article: Sanghyeok Kim *et al* 2019 *Funct. Compos. Struct.* 1 035006

View the [article online](#) for updates and enhancements.

# Functional Composites and Structures



## PAPER


# Electromechanical enhancement of metal nanoparticle thin film by composite formation with short metal nanowires

RECEIVED  
9 June 2019

REVISED  
17 August 2019

ACCEPTED FOR PUBLICATION  
17 August 2019

PUBLISHED  
10 September 2019

Sanghyeok Kim<sup>1</sup>, Jaemin Lee<sup>2</sup>, Jaeho Park<sup>1</sup>, Jung-Yong Lee<sup>2</sup>, Jae-Hyun Kim<sup>3</sup> and Inkyu Park<sup>1,4</sup> 

<sup>1</sup> Department of Mechanical Engineering, Korea Advanced Institute of Science and Technology (KAIST), Daejeon 34141, Republic of Korea

<sup>2</sup> Graduate School of Energy, Environment, Water, and Sustainability (EEWS), Korea Advanced Institute of Science and Technology (KAIST), Daejeon 34141, Republic of Korea

<sup>3</sup> Department of Nanomechanics, Nano-Convergence Mechanical System Research Division, Korea Institute of Machinery & Materials (KIMM), Daejeon 34141, Republic of Korea

<sup>4</sup> Author to whom any correspondence should be addressed.

E-mail: [inkyu@kaist.ac.kr](mailto:inkyu@kaist.ac.kr)

**Keywords:** metal nanoparticle, metal nanowire, composite thin film, printed electronics, tensile characteristics, electromechanical property

## Abstract

Recently, metal nanoparticle (NP) based ink solutions are widely used for fabricating flexible electronic devices due to many advantages such as low temperature process, simple and low-cost manufacturing, and compatibility with various flexible substrates. The electromechanical characteristics of metal NP thin films on flexible substrates are very important because they often operate under various mechanical loading conditions. Here, we report an improvement of electromechanical properties of silver (Ag) NP thin films by composite formation with short Ag nanowires (Ag NWs). We fabricated Ag NP-Ag NW hybrid thin films on the flexible polymer substrates, which presented more reliable electromechanical characteristics than the Ag NP thin film. From *in situ* scanning electron microscope images, we observed a bridging behavior of Ag NWs inhibiting the growth of cracks on the surface as well as in the inside of hybrid thin films. The improvement of electromechanical characteristics by composite formation with short Ag NWs could be also observed in the microscale line patterns, both in the static and cyclic tensile loading conditions.

## 1. Introduction

Recently, metal nanoparticle (NP) based nano-inks of silver (Ag) [1–4], copper (Cu) [4, 5], and gold (Au) [4, 6, 7] are widely used to fabricate electrodes and interconnections for flexible electronic devices. These NPs have many advantages such as simple printing and sintering processes at low temperature (~120 °C), short fabrication time (typically less than several tens of minutes), and compatibility with various substrates including rigid materials (e.g. silicon or glass) and polymer films (e.g. polyimide or polyethylene terephthalate (PET)). Also, all-solution processing without physical vapor deposition methods such as evaporation or sputtering is possible by direct printing of metal NP nano-inks [1, 2, 5–12]. For these reasons, various printed electronic devices using metal NP nano-ink such as flexible sensor [1, 2, 13–15], flexible display [16, 17], and electronic circuit [11, 18–20] have been developed.

However, mechanical failure by large deformation of metal NP thin films under elongation conditions such as stretching, bending, and twisting can be a fatal problem for the operation of printed electronic devices. Therefore, there have been studies for characterizing the mechanical properties of metal NP thin film [21–25]. In particular, solution-processed Ag NP thin film have shown poorer stretchability than the e-beam evaporated Ag thin film due to the granular microstructure with numerous pores within Ag NP thin film [25]. In addition, there have been efforts to improve the mechanical characteristics of metal NP thin films. In the work by Lee *et al* [26], the elastic modulus and yield strength of Ag NP films were improved by both forming a composite thin film with carbon nanotubes (CNTs) and using oxygen pressure controlled annealing. Also, high tensile property was

achieved by the formation of composite with very long nanowires (NWs) with length of  $\sim 95 \mu\text{m}$  [27]. However, this composite thin film is not applicable to fabricate microscale patterns with several tens of micrometers due to the large length of Ag NWs.

In this paper, we report the improvement of electromechanical characteristics of the Ag NP thin film on flexible substrates by composite formation with short Ag NWs (length =  $\sim 10 \mu\text{m}$ ). The tensile characteristics of Ag NP-NW hybrid thin films with various NW concentrations were compared with that of pure Ag NP thin films. We observed the bridging behavior by Ag NWs connecting the crack tips on the surface as well as in the inside of Ag NP-NW hybrid thin film. Also, the prevention of the crack propagation by Ag NWs aligned perpendicular to the direction of crack propagation was observed from the scanning electron microscope (SEM) imaging. In addition to the thin film, the electromechanical characteristics of the Ag NP-Ag NW hybrid line patterns under tensile strain and repetitive loading/relaxation cycles were compared with those of the pure Ag NP line patterns.

## 2. Methods

### 2.1. Fabrication process of Ag NP-Ag NW hybrid thin film

The Ag NWs were synthesized by using a polyol method [28]. The solution of synthesized Ag NWs in methanol solvent was centrifuged at 10000 rpm for 10 min to separate the Ag NWs from the solvent. After removing the solvent, Ag NWs were mixed with Ag NP ink (DGP 40LT-15C, Advanced Nano Products, Korea) using ultrasonication for 10 min. Here, the metal content and viscosity of Ag NP ink were 30 wt% and 18 cP, respectively. Then, Ag NP-Ag NW hybrid ink was spin-coated on the flexible polyimide (PI) and PET substrates as shown in figure 1. Afterwards, hybrid thin films on the substrate were sintered in a convection oven at 150 °C (on PI substrate) and at 120 °C (on PET substrate) for 30 min, respectively. After the sintering process, organic solvent was removed and then sufficient electrical conductivity could be obtained. Ag NP thin film using Ag NP ink only was also fabricated by the same coating and sintering processes.

### 2.2. Microscale line patterning of Ag NP-Ag NW hybrid thin film

Hybrid ink was spin-coated on the PI substrate and sintered in a convection oven at 150 °C for 30 min. Next, sintered hybrid thin film was ablated using a laser source with a wavelength of 1064 nm. After the laser ablation process, the sample was ultrasonicated for 1 s in order to remove the residue at the edges of the line patterns. The width and pitch of fabricated line patterns were 30  $\mu\text{m}$  and 70  $\mu\text{m}$ , respectively. Ag NP line patterns were also fabricated by the same method.

### 2.3. Tensile test and *in situ* SEM observation

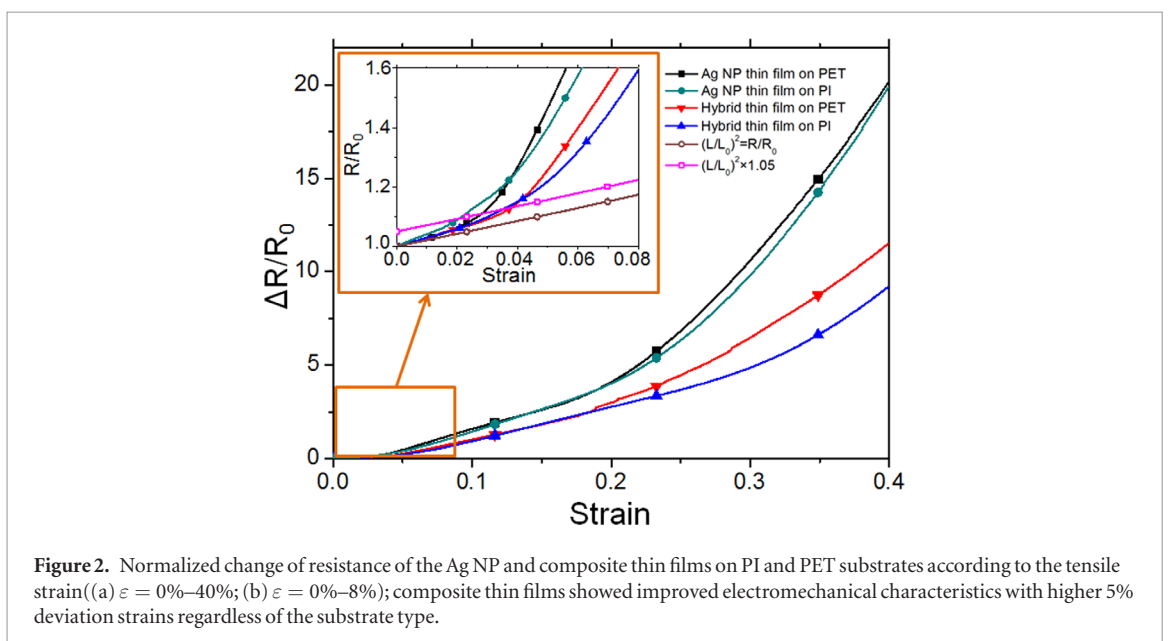
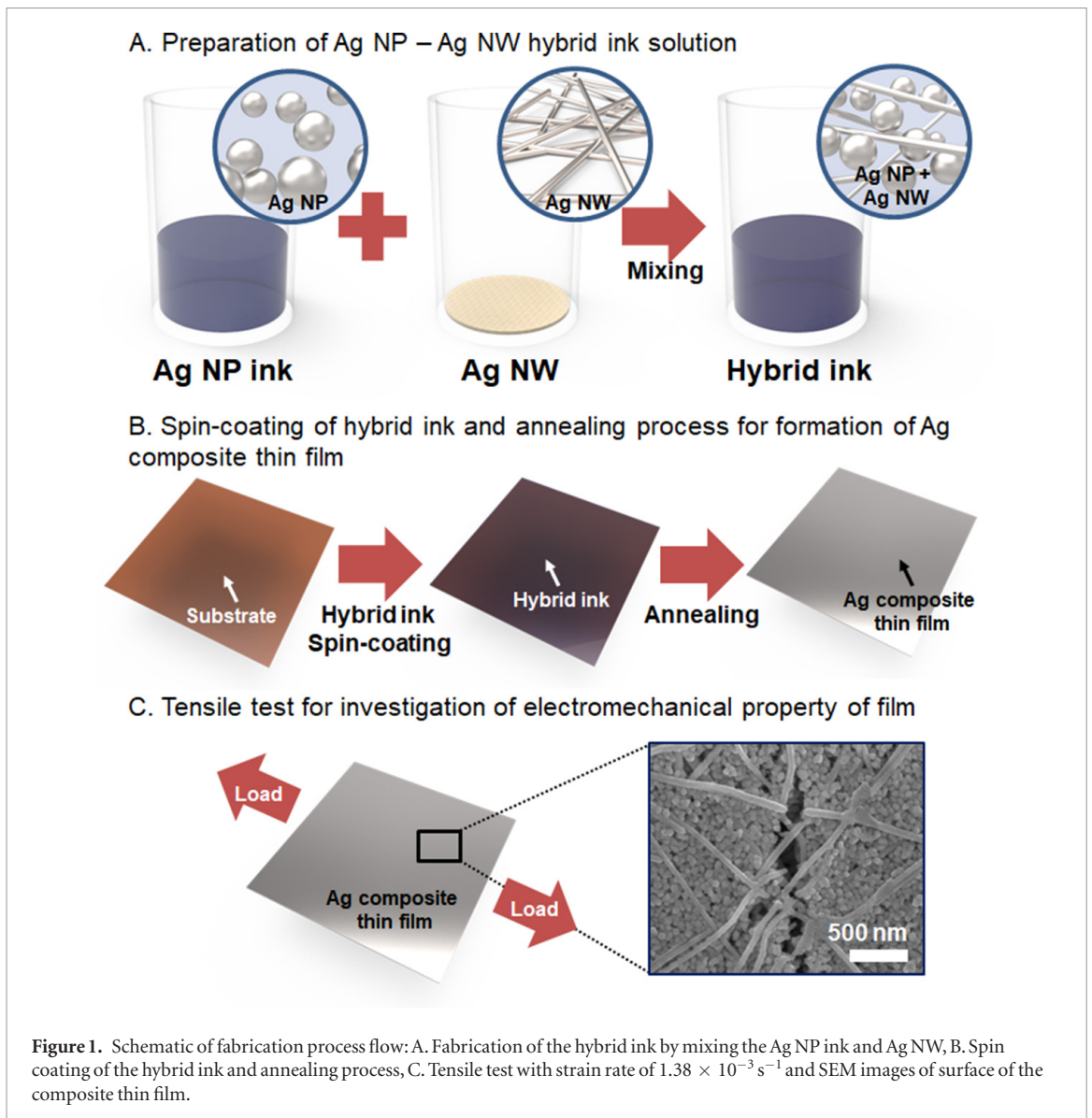
Ag NP-Ag NW hybrid and Ag NP thin films were scribed using a cutting plotter (Graphtec, Japan) for the specimens in tensile tests. The shape of the specimen was a slender rectangle with a length of 40 mm and a width of 2.5 mm. Then, tensile test was performed with a tensile tester (R&B Inc., Korea) at a strain rate of  $1.38 \times 10^{-3} \text{ s}^{-1}$ . Electrical resistances of the thin films were measured using a source meter (Keithley 2400, Keithley, USA) during the tensile test. A custom designed tensile tester was used for *in situ* observation of surface morphologies and microstructures of the elongated thin films in the SEM.

## 3. Results and discussion

The resistance-elongation curves of Ag NP and Ag NP-Ag NW hybrid thin films (Ag NW = 4 wt%; Ag NP = 96 wt%) on PI and PET substrates are shown in figure 2. During the entire elongation process, Ag NP-Ag NW hybrid thin films showed more reliable electromechanical characteristics with smaller relative change of resistance ( $\Delta R/R_0$ ) than that of the Ag NP thin film regardless of the substrate types. At a strain ( $\varepsilon$ ) of 5%,  $\Delta R/R_0$  of the Ag NP thin films on PI and PET substrates were 43% and 84% larger than those of the Ag NP-Ag NW hybrid thin films, respectively. At relatively higher strain of  $\varepsilon = 30\%$ ,  $\Delta R/R_0$  of the Ag NP thin films ( $\Delta R/R_0$  (PI) = 8.96;  $\Delta R/R_0$  (PET) = 9.72) were also 42% and 57% larger than those of the Ag NP-Ag NW hybrid thin films ( $\Delta R/R_0$  (PI) = 6.31;  $\Delta R/R_0$  (PET) = 6.20), respectively. The 5% deviation strains were measured and compared as shown in the inset of figure 2. Here, 5% deviation strain was defined as the strain when the measured change of the resistance of specimen showed 5% deviation from the following theoretical equation.

$$R/R_0 = (L/L_0)^2 \quad (1)$$

where  $L_0$  and  $R_0$  are the initial length and resistance of specimen, respectively.  $R$  is the electrical resistance of the specimen stretched to length of  $L$ . Theoretical equation (1) can be acquired by assuming a constant electrical resistivity ( $\rho$ ) and a Poisson ratio ( $\nu$ ) of 0.5 during the deformation of specimen by tensile strain [29–32]. Previous studies have verified that the crack initiation of metal thin films start at the 5% deviation strain [30, 32]. In addition, initial crack of the Ag NP thin films was confirmed around 5% deviation strain in our previous



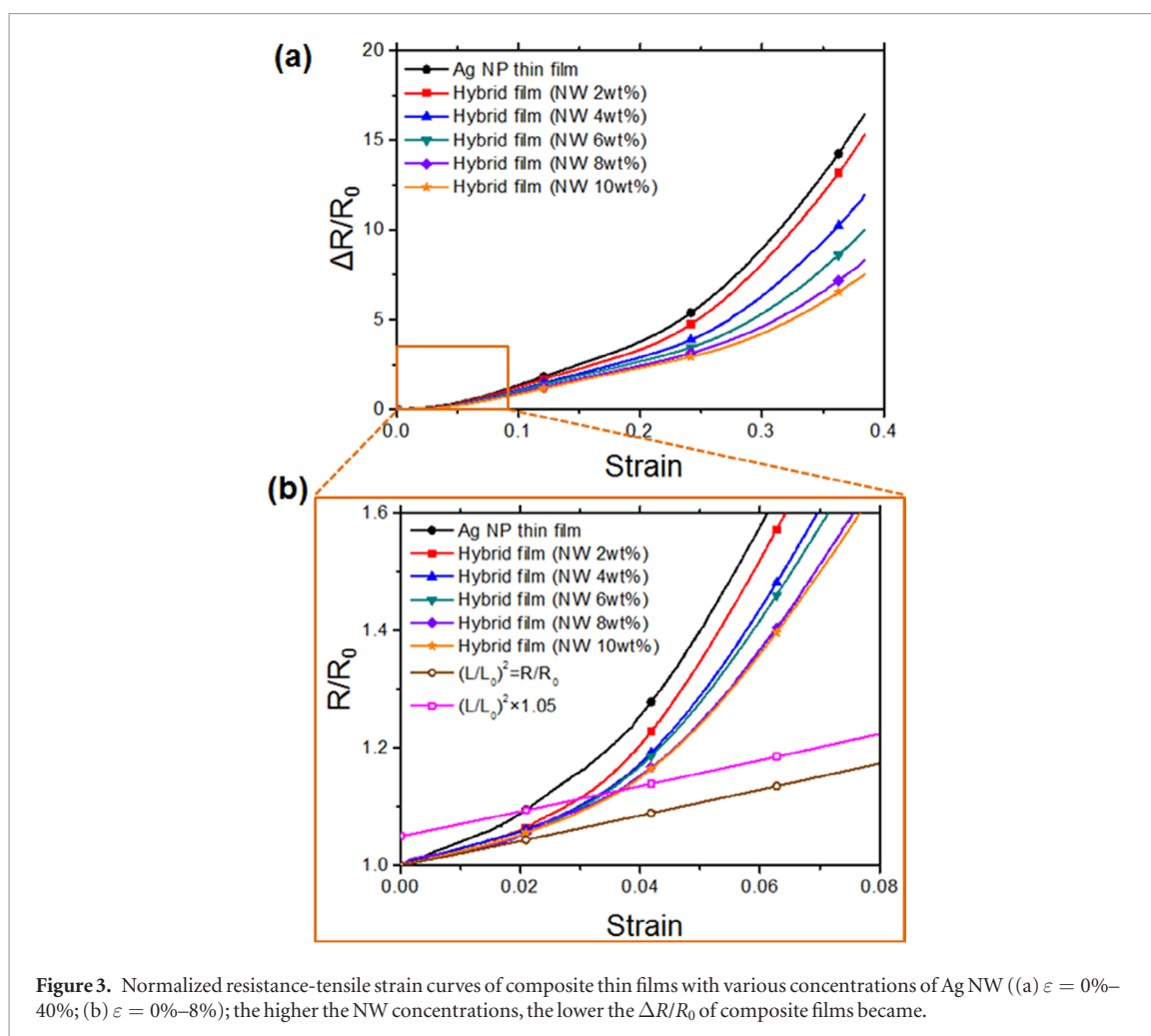


**Figure 3.** Normalized resistance-tensile strain curves of composite thin films with various concentrations of Ag NW ((a)  $\varepsilon = 0\%$ –40%; (b)  $\varepsilon = 0\%$ –8%); the higher the NW concentrations, the lower the  $\Delta R/R_0$  of composite films became.

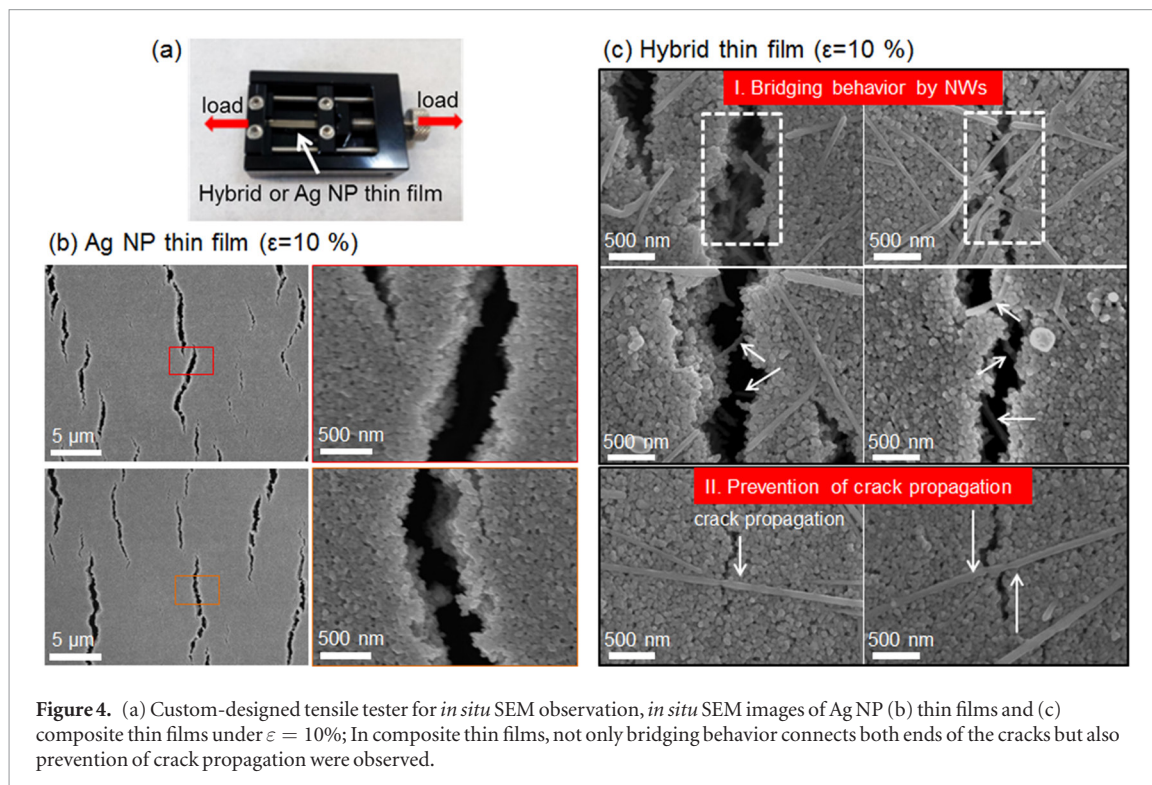
work [25]. Therefore, comparison of the 5% deviation strain can be a reasonable method to evaluate the electromechanical reliability of the metal thin films. The 5% deviation strains of the hybrid and the Ag NP thin films on the PI substrates were  $\varepsilon = 3.28\%$  (standard deviation (SD) = 0.39%) and  $\varepsilon = 2.09\%$  (SD = 0.21%), respectively. In the case of the hybrid and the Ag NP thin films on the PET substrates, the 5% deviation strains were  $\varepsilon = 3.53\%$  (SD = 0.16%) and  $\varepsilon = 2.80\%$  (SD = 0.26%), respectively. Although the differences in the 5% deviation strains were not quite significant, we verified that the electromechanical characteristics of the Ag NP thin film were improved by hybridizing with Ag NWs from the experimental results.

In addition to the substrate type, we considered the effect of concentrations of the Ag NWs. Figure 3(a) shows the resistance-elongation curves for the Ag NP-Ag NW hybrid thin films on PI substrates with various Ag NW concentrations (2–10 wt%). The higher the Ag NW concentration was, the lower  $\Delta R/R_0$  of hybrid films became. Also, the difference in the  $\Delta R/R_0$  between different Ag NW concentrations was significantly increased at higher strain. At  $\varepsilon = 35\%$ ,  $\Delta R/R_0$  of the Ag NP thin films was 13.1, which is 8.9% higher than that of the hybrid thin films with 2 wt% Ag NW ( $\Delta R/R_0 = 12.0$ ). On the other hand,  $\Delta R/R_0$  of Ag NP thin film was 118% higher than that of the hybrid film with 10 wt% Ag NW ( $\Delta R/R_0 = 5.99$ ) at  $\varepsilon = 35\%$ . Furthermore, 5% deviation strains for different Ag NW concentrations were measured and compared as shown in figure 3(b) and table 1. The 5% deviation strain was gradually increased with increasing concentration of Ag NW, resulting in a minimum and a maximum 5% deviation strain of 2.90% (SD = 0.16%) and 3.79% (SD = 0.19%) for the hybrid thin films with 2 wt% and 10 wt% Ag NW, respectively. These values were 39% and 81% higher than that of the Ag NP thin films. This result indicates that the electromechanical characteristics of the Ag NP thin films can be improved by hybridizing with Ag NWs and modulated by controlling the concentration of Ag NW.

In order to confirm why the hybridization with Ag NWs improves the electromechanical property of Ag NP thin film, *in situ* SEM observation of the hybrid thin film was conducted by increasing strains. Many previous studies have verified the improvement of mechanical characteristics by adding fibers within the composite matrix or composite films. In the works using quartz fibers [33], silicon carbide [34], and CNTs [26], the fracture

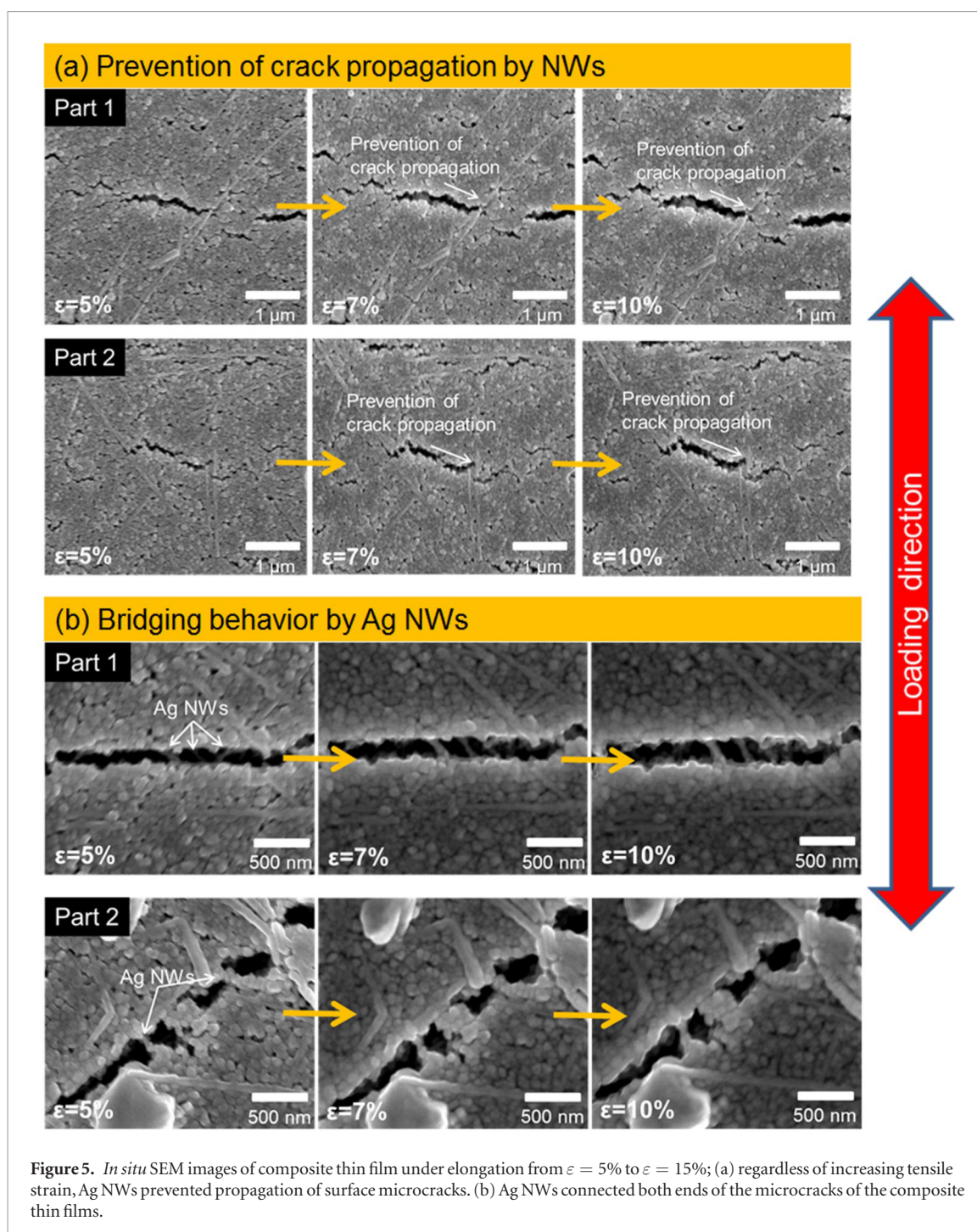
**Table 1.** Average 5% deviation strain of the composite thin films according to the concentration of Ag NW.

	Ag NW concentration (wt %)					
	0	2	4	6	8	10
Average 5% deviation strain (%)	2.09	2.90	3.28	3.46	3.72	3.79
Standard deviation (%)	0.21	0.16	0.39	0.30	0.48	0.19



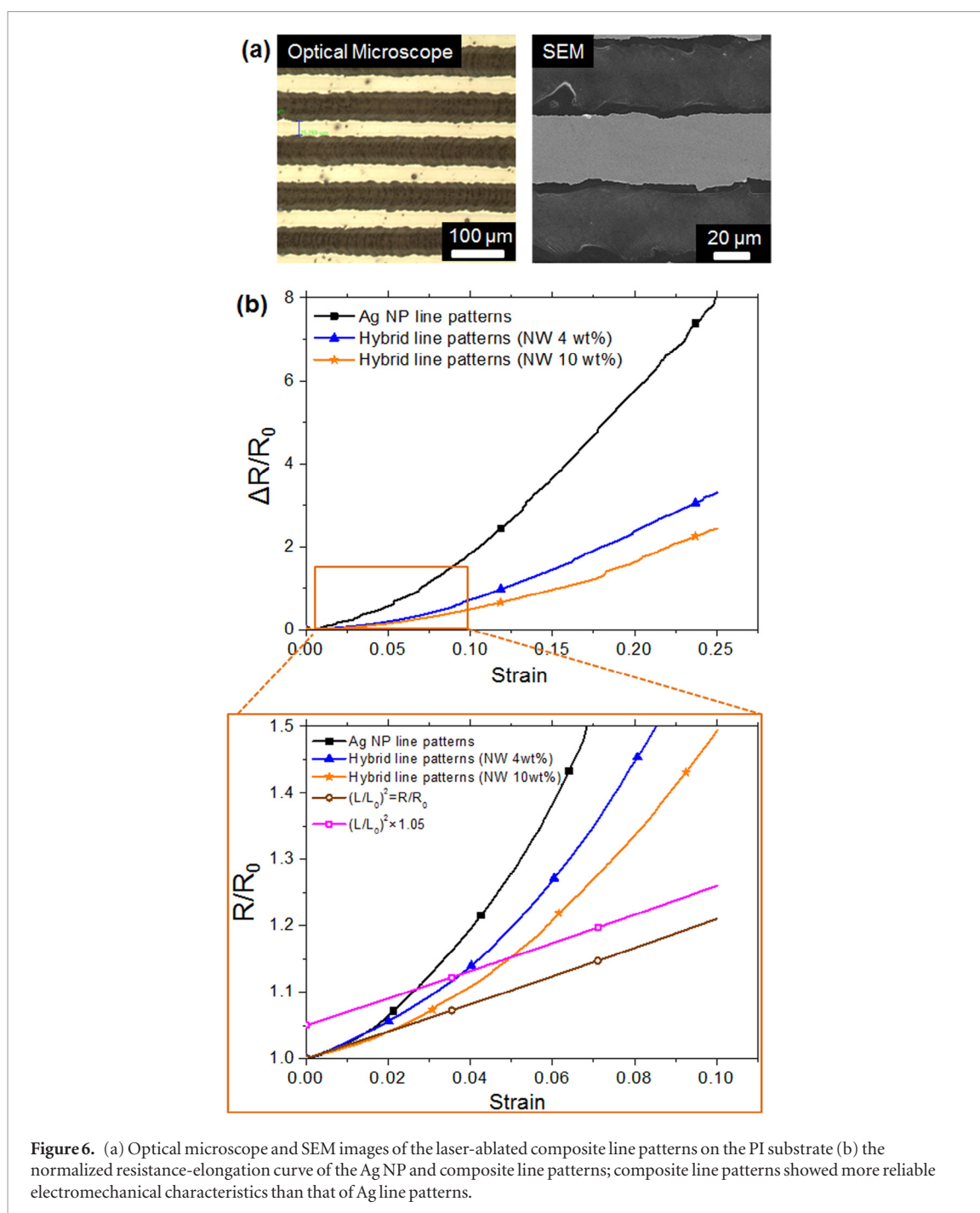
toughness of the composite matrix was improved due to the crack blockage and crack deflection by fibers. Also, the yield strength of Ag NP-CNT composite film and electromechanical property of Ag NP-long Ag NW composite film were reinforced due to the interruption of crack propagation by CNTs and nanowires, respectively. These behaviors were also observed in the present work with short Ag NWs. Figure 4 shows the *in situ* SEM images of surface cracks of the Ag NP and hybrid thin films on the PI substrates under  $\epsilon = 10\%$  by custom-designed tensile tester (see figure 4(a)). As shown in figure 4(b), a number of microcracks with size of a few hundred nanometers were formed perpendicular to the direction of tensile loading and also propagated along the grain boundaries. This behavior of crack propagation was observed and verified through atomistic computer simulation of nanocrystalline metal [21] and *in situ* TEM observation of crack propagation of freestanding Au thin film [22]. The growth and propagation of microcracks by external tensile load can cause the change of the electrical resistance of metal thin film [2]. On the other hand, two interesting phenomena were observed from the hybrid thin films under elongation ( $\epsilon = 10\%$ ). The first phenomenon is bridging behavior by Ag NWs. As shown in figure 4(c), Ag NWs connected the ends of the cracks on the surface as well as in the inside of the hybrid thin films. This bridging behavior by NWs can maintain the electrical current path as well as prevent the growth of the microcracks. The second phenomenon is the prevention of microcracks' propagation by Ag NWs. Some Ag NWs aligned perpendicular to the crack propagation on the surface of the hybrid film prevented the propagation of microcracks, resulting in the interruption of forming larger microcracks. These observations show good agreement with the behaviors that enhance the mechanical characteristics of the hybrid films. From these results, we verified why the Ag NP-Ag NW hybrid thin films have more durable and reliable electromechanical characteristics than the Ag NP thin films.

In order to analyze the growth and propagation behaviors of the microcracks and to study the hybridization effect by Ag NWs during elongation process, we observed the SEM images of the loaded Ag NP and the hybrid thin film in real time by using the *in situ* tensile jig. Figure 5 shows the *in situ* SEM images of the hybrid thin film (Ag NW = 10 wt%; Ag NP = 90 wt%;  $\epsilon = 0\% - 15\%$ ). At  $\epsilon = 5\%$ , we observed the surface microcracks formed



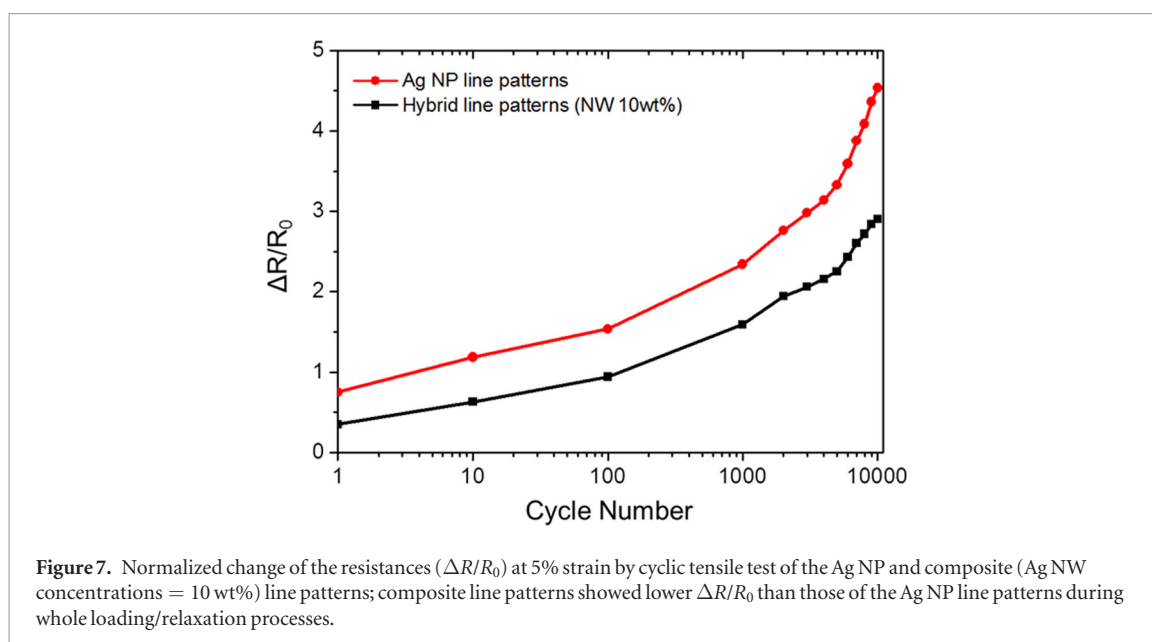
by external load and Ag NWs located on the right end of the microcrack as shown in figure 5(a). Regardless of the growth of the microcracks with increasing tensile strain, the microcrack could not propagate through the Ag NWs aligned perpendicular to the direction of the crack propagation. This behavior resulted in not only the interruption of forming larger microcrack but also the improvement electromechanical reliability. Also, as shown in figure 5(b), we observed bridging behavior by Ag NWs. At  $\epsilon = 5\%$ , Ag NWs connecting both ends of the microcracks of the hybrid thin film were observed. Regardless of the growth of the microcracks at higher tensile strain, microcracks were still connected by Ag NWs without breakage, maintaining the electrical current. From these results, we can demonstrate why the hybrid thin films have more reliable electromechanical characteristics than the Ag NP thin films.

In addition to the thin film, the effect of hybridization with Ag NWs to the electromechanical characteristics of microscale line patterns of Ag NP was investigated. Figure 6(a) shows the optical microscope and SEM images of the laser ablated Ag line patterns with width of  $30\ \mu\text{m}$  and pitch of  $70\ \mu\text{m}$ . The resistance-elongation curves by tensile test of Ag NP and Ag NP-Ag NW hybrid line patterns (Ag NW concentrations = 4 and 10 wt%) on PI



substrates are shown in figure 6(b). The hybrid line patterns showed more reliable electromechanical characteristics with the lower relative change of the resistances ( $\Delta R/R_0$ ) than those of the Ag NP line patterns. Also, the higher the Ag NW concentration was, the lower  $\Delta R/R_0$  of the hybrid line patterns became. The 5% deviation strains of the Ag NP line patterns were 2.60% (SD = 0.27%). On the other hand, the 5% deviation strains of the Ag NP-Ag NW hybrid line patterns were 3.75% (SD = 0.25%) and 4.78% (SD = 0.19%) for 4 wt% Ag NW and 10 wt% Ag NW, respectively. From these results, we verified that hybridization of Ag NP-Ag NW improved the electromechanical reliability of both thin films and microscale line patterns. Furthermore, in order to investigate the mechanical robustness of the Ag NP and hybrid line patterns as the electrical interconnection, we performed cyclic tensile tests by repeated loading and relaxation. Repeated cycles of tensile strain between  $\varepsilon = 1\%$  and  $\varepsilon = 5\%$  was conducted by 10 000 times. Relative changes of the resistances ( $\Delta R/R_0$ ) at 5% strain in increasing loading/relaxation cycles were compared as shown in figure 7. The hybrid line patterns showed lower  $\Delta R/R_0$  than those of the Ag NP line patterns. After 10 000 cycles,  $\Delta R/R_0$  of the hybrid line pattern and Ag NP line pattern were 2.90 and 4.53, respectively. This result indicates the improved mechanical reliability of Ag NP thin film by hybridization with Ag NWs due to the inhibition of crack propagation and bridging effect by Ag NWs.





#### 4. Conclusion

In summary, we investigated the electromechanical characteristics of Ag NP-Ag NW hybrid thin films on flexible polymer substrates and compared with those of Ag NP thin films by measuring the electrical resistance under tensile strain. Hybrid thin films showed improved electromechanical properties than those of Ag NP thin films. From the *in situ* SEM observation, we verified that the mechanical reliability of hybrid thin film was improved by the bridging behavior of Ag NWs that connect the microcracks as well as by the inhibition of the crack propagation with Ag NWs. It is believed that this work can provide a better understanding of the hybridizing effect by short Ag NWs on the mechanical characteristics of metal NP-NW hybrid film and can help the fabrication of flexible printed electronic devices with improved mechanical reliability.

#### Acknowledgments

This work was supported by (1) Nano-Convergence Foundation ([www.nanotech2020.org](http://www.nanotech2020.org)) funded by the Ministry of Science and ICT (MSIT, Korea) and the Ministry of Trade, Industry and Energy (MOTIE, Korea) [Project number: R201603110] and (2) National Research Foundation of Korea (NRF) grant funded by the Ministry of Science and ICT (MSIT, Korea) (No. 2018R1A2B2004910).

#### ORCID iDs

Inkyu Park  <https://orcid.org/0000-0001-5761-7739>

#### References

- [1] Kim S, Lee W S, Lee J and Park I 2012 Direct micro/nano metal patterning based on two-step transfer printing of ionic metal nano-ink *Nanotechnology* **23** 285301
- [2] Lee J, Kim S, Lee J, Yang D, Park B C, Ryu S and Park I 2014 A stretchable strain sensor based on a metal nanoparticle thin film for human motion detection *Nanoscale* **6** 11932–9
- [3] Mo L, Guo Z, Yang L, Zhang Q, Fang Y, Xin Z, Chen Z, Hu K, Han L and Li L 2019 Silver nanoparticles based ink with moderate sintering in flexible and printed electronics *Int. J. Mol. Sci.* **20** 2124
- [4] Kamyshny A and Magdassi S 2019 Conductive nanomaterials for 2D and 3D printed flexible electronics *Chem. Soc. Rev.* **48** 1712–40
- [5] Norman A L, Evagelos K A and Wendelin J S 2008 Graphene-stabilized copper nanoparticles as an air-stable substitute for silver and gold in low-cost ink-jet printable electronics *Nanotechnology* **19** 445201
- [6] Park I, Ko S H, Pan H, Grigoropoulos C P, Pisano A P, Fréchet J M J, Lee E S and Jeong J H 2008 Nanoscale patterning and electronics on flexible substrate by direct nanoimprinting of metallic nanoparticles *Adv. Mater.* **20** 489–96
- [7] Ko S H, Park I, Pan H, Grigoropoulos C P, Pisano A P, Luscombe C K and Fréchet J M J 2007 Direct nanoimprinting of metal nanoparticles for nanoscale electronics fabrication *Nano Lett.* **7** 1869–77
- [8] Kim S, Park J H, Kang K, Park C O and Park I 2015 Direct metal micropatterning on needle-type structures towards bioimpedance and chemical sensing applications *J. Micromech. Microeng.* **25** 015002
- [9] Kim E U, Baeg K J, Noh Y Y, Kim D Y, Lee T, Park I and Jung G Y 2009 Templated assembly of metal nanoparticles in nanoimprinted patterns for metal nanowire fabrication *Nanotechnology* **20** 355302

- [10] Bai S, Zhang S, Zhou W, Ma D, Ma Y, Joshi P and Hu A 2017 Laser-assisted reduction of highly conductive circuits based on copper nitrate for flexible printed sensors *Nano-Micro Lett.* **9** 42
- [11] Balliu E, Andersson H, Engholm M, Öhlund T, Nilsson H E and Olin H 2018 Selective laser sintering of inkjet-printed silver nanoparticle inks on paper substrates to achieve highly conductive patterns *Sci. Rep.* **8** 10408
- [12] Raut N C and Al-Shamery K 2018 Inkjet printing metals on flexible materials for plastic and paper electronics *J. Mater. Chem. C* **6** 1618–41
- [13] Abu-Khalaf J M, Al-Ghussain L and Al-Halhouli A 2018 Fabrication of stretchable circuits on polydimethylsiloxane (PDMS) pre-stretched substrates by inkjet printing silver nanoparticles *Materials* **11** 1–17
- [14] Lee G Y, Kim M S, Yoon H S, Yang J, Ihn J B and Ahn S H 2017 Direct printing of strain sensors via nanoparticle printer for the applications to composite structural health monitoring *Proc. CIRP* **66** 238–42
- [15] Park Y, Lim S, Jeong S, Song Y, Bae N, Hong S, Choi B, Lee S and Lee K 2018 Flexible nanopillar-based electrochemical sensors for genetic detection of foodborne pathogens *Nano Converg.* **5** 15
- [16] Wood V, Panzer M J, Chen J, Bradley M S, Halpert J E, Bawendi M C and Bulović V 2009 Inkjet-printed quantum dot-polymer composites for full-color AC-driven displays *Adv. Mater.* **21** 2151–5
- [17] Shen W, Zhang X, Huang Q, Xu Q and Song W 2014 Preparation of solid silver nanoparticles for inkjet printed flexible electronics with high conductivity *Nanoscale* **6** 1622–8
- [18] Jo J, Yu J S, Lee T M and Kim D S 2009 Fabrication of printed organic thin-film transistors using roll printing *Jpn. J. Appl. Phys.* **48** 04C181
- [19] Park M et al 2012 Highly stretchable electric circuits from a composite material of silver nanoparticles and elastomeric fibres *Nat. Nanotechnol.* **7** 803–9
- [20] Ko S H, Park I, Pan H, Misra N, Rogers M S, Grigoropoulos C P and Pisano A P 2008 ZnO nanowire network transistor fabrication on a polymer substrate by low-temperature, all-inorganic nanoparticle solution process *Appl. Phys. Lett.* **92** 154102
- [21] Farkas D, Van Swygenhoven H and Derlet P M 2002 Intergranular fracture in nanocrystalline metals *Phys. Rev. B* **66** 601011–4
- [22] Wang H, Nie A, Liu J, Wang P, Yang W, Chen B, Liu H and Fu M 2011 In situ TEM study on crack propagation in nanoscale Au thin films *Scr. Mater.* **65** 377–9
- [23] Herrmann J, Müller K H, Reda T, Baxter G R, Raguse B, De Groot G J J B, Chai R, Roberts M and Wiczorek L 2007 Nanoparticle films as sensitive strain gauges *Appl. Phys. Lett.* **91** 183105
- [24] Lee I, Kim S, Yun J, Park I and Kim T S 2012 Interfacial toughening of solution processed Ag nanoparticle thin films by organic residuals *Nanotechnology* **23** 485704
- [25] Kim S, Won S, Sim G-D, Park I and Lee S-B 2013 Tensile characteristics of metal nanoparticle films on flexible polymer substrates for printed electronics applications *Nanotechnology* **24** 085701
- [26] Lee J H, Kim N R, Kim B J and Joo Y C 2012 Improved mechanical performance of solution-processed MWCNT/Ag nanoparticle composite films with oxygen-pressure-controlled annealing *Carbon* **50** 98–106
- [27] Lee I, Lee J, Ko S H and Kim T S 2013 Reinforcing Ag nanoparticle thin films with very long Ag nanowires *Nanotechnology* **24** 415704
- [28] Lee J, Lee I, Kim T S and Lee J Y 2013 Efficient welding of silver nanowire networks without post-processing *Small* **9** 2887–94
- [29] Lu N, Wang X, Suo Z and Vlassak J 2009 Failure by simultaneous grain growth, strain localization, and interface debonding in metal films on polymer substrates *J. Mater. Res.* **24** 379–85
- [30] Sim G D, Won S, Jin C Y, Park I, Lee S B and Vlassak J J 2011 Improving the stretchability of as-deposited Ag coatings on poly-ethylene-terephthalate substrates through use of an acrylic primer *J. Appl. Phys.* **109** 073511
- [31] Lu N, Wang X, Suo Z and Vlassak J 2007 Metal films on polymer substrates stretched beyond 50% *Appl. Phys. Lett.* **91** 221909
- [32] Lu N, Suo Z and Vlassak J J 2010 The effect of film thickness on the failure strain of polymer-supported metal films *Acta Mater.* **58** 1679–87
- [33] Li C, Chen Z, Zhu J, Liu Y, Jiang Y, Guan T, Li B and Lin L 2012 Mechanical properties and microstructure of 3D orthogonal quartz fiber reinforced silica composites fabricated by silicasol-infiltration-sintering *Mater. Des.* **36** 289–95
- [34] Guicciardi S, Silvestroni L, Nygren M and Sciti D 2010 Microstructure and toughening mechanisms in spark plasma-sintered ZrB<sub>2</sub> ceramics reinforced by SiC whiskers or SiC-chopped fibers *J. Am. Ceram. Soc.* **93** 2384–91